Journal of APPLIED PHYSICS

Volume 60 1 August 1986 Number 3

Applied Physics Review:
Atomic layer epitaxy
by Colin H. L. Goodman and Markus V. Pessa

a publication of the American Institute of Physics

0021-8979(19860801)60:3-0

CODEN: JAPIAU

ISSN: 0021-8979

Journal of APPLIED PHYSICS

The *Journal of Applied Physics* is published semimonthly by the American Institute of Physics (AIP) with the cooperation of The American Physical Society. It is devoted to general physics and its applications to other sciences, to engineering, and to industry. (Prior to 1937, the Journal carried the name *Physics.*) The Editor welcomes manuscripts describing significant new experimental or theoretical results in applied physics or manuscripts concerning important new applications of physics to other branches of science and engineering.

Information for Contributors

Submit manuscripts to Lester Guttman, Editor, *Journal of Applied Physics,* Argonne National Laboratory, P.O. Box 296, Argonne, IL 60439. Submission is a representation that the manuscript has not been published previously nor currently submitted for publication elsewhere. The manuscript should be accompanied by a statement transferring copyright from the authors (or their employers—whoever holds the copyright) to AIP; a suitable form for copyright transfer is occasionally printed in the back of this journal and is available from the Editor's office or AIP. This written transfer of copyright, which previously was assumed to be implicit in the act of submitting a manuscript, is necessary under the 1978 U.S. copyright law in order for AIP to continue disseminating physics research results as widely as possible. Further information may be obtained from AIP.

Publication Charge: To support the cost of wide dissemination of research results through publication of journal pages and production of a data base of articles, the author's institution is requested to pay a *page charge* of $45 per page (with a one-page minimum) and an *article charge* of $20 per article. The page charge (if honored) entitles the author to 100 free reprints. For **Errata** the minimum page charge is $10, with no article charge and no free reprints. Nonpayment of the publication charge may lead to delays in publication.

Two categories of manuscripts are acceptable, **full-length articles** and **Communications.** The latter are short contributions not generally exceeding in length nine double-spaced typewritten pages or approximately 2500 words of text reduced, however, by allowances for equations, tables, and figures. Abstracts are required for manuscripts of both types. Being short, Communications are often published more quickly than full-length articles. Instructions for preparation of **manuscripts** will be found in the January issue of this journal and occasionally in later issues. In brief and incomplete summary: Two copies of the manuscript, including clear copies of the figures, are required, double-spaced throughout on one side of 21.6×28 cm ($8\frac{1}{2}\times11$ in.) paper. The original should be retained by the author until it is requested, after review. The *abstract, references, figure captions,* and *tables* are similarly to be double-spaced each on its separate sheets. The original *figures* should be original line drawings or high-contrast glossy prints not larger than 21.6×28 cm and should be included with the original submission. *References* should conform to the style used in AIP journals including this one. Unusual mathematical symbols should be clarified with marginal notes.

AIP's **Physics Auxiliary Publication Service (PAPS)** is a low-cost depository for material which is part of and supplementary to a published paper, but is too long to be included in the journal; inquire of the Editor.

Proofs and all correspondence concerning papers in the process of publication should be addressed to: Editorial Supervisor, *The Journal of Applied Physics,* American Institute of Physics, 335 East 45th Street, New York, NY 10017. In all correspondence reference should be made to title, author, journal, and scheduled date of issue. A limited number of **alterations in proof** are unavoidable, but the cost of making extensive alterations after the article has been set in type will be charged to the author.

Second-class postage rates paid at Woodbury, N.Y. and at additional mailing offices

6/1/86

ABOUT THAT BAR CODE

No, the *Journal of Applied Physics* is not being sold in supermarkets. The bar code on our cover is there because AIP, along with other publishers, is participating in a test sponsored by the Serials Industry Systems Advisory Committee (SISAC). The test will run through October 1986. Our hope is that the bar code will be of assistance to libraries in serials check-in, circulation control, and reprint ordering. For those interested, the code used is Code 128. We welcome comments from libraries and other subscribers on this new service.

(Continued)

Subscription Prices (1986)	U.S.A. & Poss.	Foreign (incl. Can. & Mex.)	Optional air freight: Europe, Mideast, N. Africa	Optional air freight: Asia & Oceania	Microfiche (1st class/airmail)
Members*	$80.00	$130.00	$187.00	$280.00	$80.00
Reg. rate	$495.00	$545.00	$602.00	$695.00	$495.00

*AIP Member and Affiliated Societies.

Back-Number Prices. Single copies from Vol. 24 (1953) through Vol. 55 (1984): $35.00; Vol. 56 (1984) and thereafter: $22.00. Special Supplements: $50.00. Volumes 1–23 (1931–1952) are available only on microfilm.

The *Journal of Applied Physics* (ISSN: 0021-8979) is published semimonthly by the American Institute of Physics, 500 Sunnyside Blvd., Woodbury, NY 11797. Second-class postage paid at Woodbury, NY, and additional mailing offices. POSTMASTER: Send address changes to *Journal of Applied Physics*, 500 Sunnyside Blvd., Woodbury, NY 11797.

Subscriptions, renewals, address changes, and single-copy orders should be addressed to *AIP Subscription Fulfillment Division, 335 East 45th St., New York, NY 10017*. Allow at least six weeks advance notice. For address changes please send both old and new addresses and, if possible, include a mailing label from the wrapper of a recent issue. For your convenience a **change of address form is included in every issue of *Physics Today*; please use it.** Requests from subscribers for missing journal issues will be honored without charge only if received within six months of the issue's actual date of publication; otherwise, the issue may be purchased at the single-copy price. (AIP Headquarters are located at 335 East 45th St., New York, NY 10017; Subscription Fulfillment offices are located at 500 Sunnyside Blvd., Woodbury, NY 11797.)

Reprints of individual articles in this journal may be ordered singly at $10.00 per article copy (postage included) for articles up to 20 pages. Beyond 20 pages there is a surcharge of $0.20 per page. Air mail delivery is available. Orders are filled within one week of receipt or of the date of publication, whichever is later. Send orders to the American Institute of Physics, *Current Physics Reprints*, 335 East 45th St., New York, NY 10017.

Copying Fees: The code that appears on the first page of articles in this journal gives the fee for each copy of the article made beyond the free copying permitted by AIP. (See statement under "Copyright" elsewhere in this journal.) If no code appears, no fee applies. The fee for pre-1978 articles is $0.25 per copy. With the exception of copying for advertising and promotional purposes, the express permission of AIP is not required provided the fee is paid through the *Copyright Clearance Center, Inc. (CCC), 21 Congress St., Salem, MA 01970.* Contact the CCC for information on how to report copying and remit payment.

Microfilm subscriptions of complete volumes of the *Journal of Applied Physics* are available on 16 mm and 35 mm. The *Journal of Applied Physics* also appears on a monthly basis in *Current Physics Microform* (CPM) Section 1 along with 25 other journals published by the American Institute of Physics and its member societies. A *Microfilm Catalog* is available on request. The *Journal of Applied Physics* is indexed quarterly in *Current Physics Index*, a subject and author index (with abstracts) to all journals published by AIP and its member societies.

CONDENSED MATTER: Structure, Mechanical, and Thermal Properties (PACS 61–68)

CONDENSED MATTER: Electrical and Magnetic Properties (PACS 71–76)

(Continued)

(Continued)

ERRATUM

iv

Atomic layer epitaxy

Colin H. L. Goodman
Standard Telecommunication Laboratories, Harlow, Essex, England

Markus V. Pessa
Department of Physics, Tampere University of Technology, SF-33101 Tampere, Finland

(Received 4 November 1985; accepted for publication 31 March 1986)

Atomic layer epitaxy (ALE) is not so much a new technique for the preparation of thin films as a novel modification to existing methods of vapor-phase epitaxy, whether physical [e.g., evaporation, at one limit molecular-beam epitaxy (MBE)] or chemical [e.g., chloride epitaxy or metalorganic chemical vapor deposition (MOCVD)]. It is a self-regulatory process which, in its simplest form, produces one complete molecular layer of a compound per operational cycle, with a greater thickness being obtained by repeated cycling. There is no growth *rate* in ALE as in other crystal growth processes. So far ALE has been applied to rather few materials, but, in principle, it could have a quite general application. It has been used to prepare single-crystal overlayers of CdTe, (Cd,Mn)Te, GaAs and AlAs, a number of polycrystalline films and highly efficient electroluminescent thin-film displays based on ZnS:Mn. It could also offer particular advantages for the preparation of ultrathin films of precisely controlled thickness in the nanometer range and thus may have a special value for growing low-dimensional structures.

TABLE OF CONTENTS

I. INTRODUCTION

Thin films are of the greatest technological importance, and range widely in application: the active layers in semiconductor devices as well as the dielectrics in them or in electrolytic capacitors, the transparent conductors in liquid-crystal displays or on aircraft windshields, the luminescent and protective layers in electroluminescent (EL) thin-film displays, etc. More recently ultrathin films of uniform and precisely controlled thickness in the range 1–10 nm have come to be of the greatest importance both scientifically in the branch of solid-state physics termed "low-dimensional," as well as technologically in integrated circuits and optoelectronic devices.

In this general context little attention was initially paid to a patent of Finnish origin taken out in 1977[1] which described a novel mode of evaporation deposition, atomic layer epitaxy (ALE), for preparing thin films of zinc sulfide. This originated from the Lohja Corporation but was probably too unorthodox and seemingly restricted in application to make much impact. By 1980, however, it was being used to make remarkably good large-area thin-film EL displays based on ZnS:Mn (Refs. 2 and 3), and in 1982 still better displays from Lohja won, against strong U.S. and Japan competition, the prize of the Society of Information Display for the greatest advance in the display field during the preceeding year. ALE began to attract considerable attention as a method for producing thin films of high quality. More recently still, with the epitaxial film work of Pessa's group at Tampere University of Technology, Finland, on II-VI compounds, and of Nishizawa's group at Tohoku University, Japan, on gallium arsenide, as well as works of Usui *et al.* at Nippon Electric Corporation and Bedair *et al.* at North Carolina State University, on GaAs, the promise of ALE for growing low-dimensional structures has generated much interest.

II. FILM GROWTH BY ATOMIC LAYER EPITAXY

A particularly simple way to describe the ALE approach is to say that it makes use of the difference between chemical absorption and physical adsorption. When the first layer of atoms or molecules of a reactive species reaches a solid surface there is usually a strong interaction (chemisorption); subsequent layers tend to interact much less strongly (physisorption). If the initial substrate surface is heated sufficiently one can achieve a condition such that only the chemisorbed layer remains attached. In the earliest and perhaps simplest example of ALE, viz., the growth of ZnS by evaporation in a vacuum, Zn vapor was allowed to impinge on the heated glass. Evaporation was then stopped and if physisorbed Zn were present because of the impinging flux, it would reevaporate. The process was then repeated with sulfur, the first layer of which would chemisorb on the initial Zn layer; any subsequent physisorbed sulfur would gradually come away from the heated substrate when the

 0021-8979/86/150R65-17$02.40

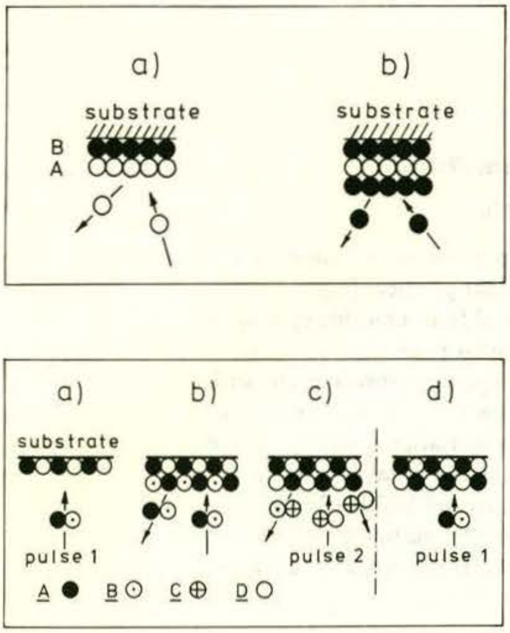

FIG. 1. Film growth by ALE. Upper panel: growth from elemental source materials [variant (i)]. Lower panel: growth from compound source materials via surface exchange reactions [variant (ii)].

sulfur flux was cut off, leaving one (double) layer of ZnS. This complete cycle could be repeated indefinitely, the number of layers grown being determined solely by the number of cycles [see Fig. 1(a)]. This cyclic vacuum evaporation was described in the original Lohja patent.[1]

It has been shown by straightforward measurements[4] that chemical vapor deposition (CVD) of ZnS from $ZnCl_2$ and H_2S could also be operated in an ALE mode, the cycle being somewhat more complex [Fig. 1(b)] in that a chemisorbed $ZnCl_2$ monolayer loses its chlorine to the hydrogen of the later-arriving H_2S molecules, forming HCl, and again resulting in a (double) layer of ZnS. The importance of this CVD variant is that it enables ALE to be applied to compounds with one or more involatile constituents for which the evaporative approach would clearly not be viable.

One can thus arrive at a definition of ALE: it is based on chemical reactions at the solid surface of a substrate, to which the reactants are transported alternately as pulses of neutral molecules or atoms, either as chopped beams in high vacuum, or as switched streams of vapor possibly on an inert carrier gas. The incident pulse reacts directly and chemically only with the outermost atomic layer of the substrate. The film therefore grows stepwise—a single monolayer per pulse—provided that at least one complete monolayer coverage of a constituent element, or of a chemical compound containing it, is formed before the next pulse is allowed to react with the surface. Given that, any excess incident molecules or atoms impinging on the film do not stick if the substrate temperature T_{gr} is properly chosen, and one therefore obtains precisely a monolayer coverage in each cycle.

The formation of a "layer per cycle" is the specific feature that conceptually distinguishes the ALE mode from other modes of vapor phase deposition; the latter all give a growth rate, ALE gives a growth per cycle.

Some confusion appears to have been generated because the ALE-grown materials actually used by Lohja in their displays were polycrystalline or amorphous. Also it was not easy from what was published to deduce experimental conditions. It was only later that the first controlled experiments in a laboratory environment[4,5] were carried out at the Tampere University of Technology in 1979–80, and provided confirmation of the general correctness of the ideas developed by Suntola at Lohja. These were followed by further experiments involving deposition onto single-crystal substrates, discussed later in Sec. IV. These experiments showed that the idealized ALE picture, of one complete double layer being grown per cycle, could be an oversimplification. As discussed subsequently, incomplete layer growth occurs in many cases.

To sum up the present situation: the ALE mode of deposition has so far only been applied to a rather small number of materials, listed in detail in Sec. IV. These materials are of considerable scientific and technological interest. It seems highly probable, though yet unproved, that a very much wider range of materials could be handled. One particularly remarkable feature claimed for the ALE approach is that it automatically gives an absolute control of deposit thickness in terms of the number of cycles employed. However, although the general conditions under which ALE would be possible seem reasonable clear, each material will have its own specific requirements regarding the operational conditions under which deposits of high perfection and purity could be obtained—while in some cases ALE might turn out not to be applicable.

III. THEORETICAL ASPECTS

A. Growth models

As already indicated ALE in its basic form operates by growing complete atomic layers on top of each other, there being two basic variants based on (i) evaporative deposition [with as one extreme, molecular-beam epitaxy (MBE)], relying on heated elemental source materials, or (ii) chemical vapor deposition (CVD), relying on sequential surface exchange reactions between compound reactants.

ALE, therefore, is not so much an entirely new method of crystal growth as a special mode of these well-established growth techniques.

Both ALE variants, illustrated in Fig. 1, assume that at the substrate temperature the vapor pressures of the source materials as solid phases are much larger, perhaps by several orders of magnitude, than those of the compound films eventually formed from them. This requirement is usually met in the case of II-VI materials and can hold reasonably well in many other cases.

The precaution must be taken to turn off the source beam for a sufficiently long time (of the order of 1 s) after each deposition pulse. In this way the surface is allowed to approach thermodynamic equilibrium at the end of each reaction step—a growth condition that is not usually met in other techniques of deposition by evaporation. It is then clear that the fluid dynamics are entirely eliminated from the growth problem. We should also note that a low net growth rate, a characteristic of ALE, can be partly compensated by designing reactors properly to allow for depositing several large-area samples simultaneously (such a reactor is illustrated in Fig. 4; see Sec. IV).

In ALE variant (i), element A and element B are alternately deposited onto the substrate at temperature T_{gr}. The number of monolayers produced by one pulse can be calculated from

$$\theta = (I_i - I_e)t_i/\theta_i.$$

Here θ_i is the atomic density for one monolayer coverage ($\theta = 1$), I_i the number of atoms per second impinging on the substrate of unit area, I_e the number of atoms per second reevaporated from the substrate during deposition, and t_i the duration of the pulse. As θ reaches unity the sticking coefficient abruptly changes from unity to zero; i.e., I_e becomes equal to I_i. Only a monolayer of element A held by strong B–A bonds is left behind after reevaporation of those atoms (or molecules) that are present in excess. Next, the surface is subjected to a pulse of B. Once all possible A–B bonds have formed, no further B will stick. The process is repeated with alternate pulses of A and B until the desired film thickness is achieved, one monolayer at a time.

Such behavior can be termed the ideal ALE mode.[6] Experiments, however, indicate that this model is oversimplified because it does not take into account the fact that perfect layer-by-layer growth does not always take place, even if an optimum value of T_{gr} is chosen. A detailed study of growth of CdTe epilayers on CdTe (111) substrates has shown[7] that the sticking coefficients of Cd and Te are less than unity at T_{gr}. The persistent coverages left behind after reevaporation are measured to be only 35% of a monolayer for Cd on CdTe (111)B and 72% for Te on CdTe(111)A. Such coverages have structural implications—see the discussion in Sec. III B.

A generalized model has been suggested[7] for growth of an AB compound by ALE variant (i) which involves (a) the existence of weakly bound states of both reactants in the vicinity of the interface and (b) partial reevaporation of the first elemental monolayer deposited. According to this model, the timing and dose of the sequential pulses of elemental A and B should be carefully related to each other. This, of course, represents a considerable departure from the ideal ALE model but does retain the basic growth per cycle that is *the* distinctive feature of ALE.

In the case of ALE variant (ii), sequential surface exchange reactions are used to grow a film of a compound AD [see Fig. 1(b)]. During the first phase of a deposition cycle incident molecules AB are adsorbed by the surface layer. AB remains on the surface until a pulse of CD molecules arrives. At a properly chosen T_{gr} the surface reaction $AB + CD \rightarrow BC + AD$ then occurs. This releases B and C (usually as a compound BC) and results in the formation of a layer of AD. As with ALE variant (i), the growth proceeds stepwise, and is independent of the size of a reactant pulse, provided that it exceeds the minimum amount of material required to form the appropriate adsorbed monolayer. It nonetheless appears probable that, as noted for variant (i), the timing and dose of sequential pulses would need to be related to each other.

Comprehensive theoretical quantum chemical studies of the growth of a ZnS surface by ALE variant (ii) using the first of these reactions have been carried out by Pakkanen *et al.*[8] These studies showed that the growth process, which involves several reaction steps, again is not so simple as the ideal ALE reaction scheme shown in Fig. 1b. The calculations were based on *ab initio* Hartree–Fock theory for atoms and molecules. They showed that the formation of a complete ZnS overlayer does not occur in a single ALE cycle.

The calculations suggest that two different growth mechanisms could occur involving ALE-type cyclic reaction with molecules of $ZnCl_2$ and H_2S. These mechanisms might operate simultaneously at different sites of the real ZnS surface. In the first of these mechanisms surface chains are formed, the first step in this chain process being the chemisorption of $ZnCl_2$ which produces a chlorine-bridged $ZnCl_2$ overlayer with a maximum surface coverage of 0.5. Subsequent H_2S adsorbates react with the $ZnCl_2$ chains releasing HCl and creating ZnS chains with the S atoms at the top. $ZnCl_2$ molecules of the next pulse bind to the S atoms and again form a chlorine-bridged $ZnCl_2$ overlayer with a surface coverage of 0.5. The second H_2S pulse completes the new ZnS layer. This complete layer is identical to the bulk structure. On this basis, the maximum growth rate is one new layer per two cycles of $ZnCl_2 + H_2S$. In the second mechanism, an alternative, somewhat similar set of reactions was proposed for the formation of $ZnCl_2$-ring overlayers. The initial surface coverage would now be 0.33 and the maximum growth rate would therefore become one ZnS layer per three cycles of $ZnCl_2 + H_2S$.

Deviations from the simple model of ALE growth discussed so far have all indicated a reduction of the thickness grown per cycle. However, some recently published work[9,10] on GaAs grown by ALE variant (ii), and discussed in Section IV A 3, indicates that growth can proceed in a complete layer-by-layer fashion; in some circumstances there can even be an increase of the thickness per cycle.[11]

B. Kinetic effects

Several factors must be satisfied for ALE growth to be possible. ALE implies the need for (a) a flat perfect substrate surface and (b) equally strong adsorption of the two vapor species taking part in the cycle, and equally easy desorption of any reaction products in the case of ALE variant (ii). It does not as yet appear possible to calculate *accurately* to what extent these requirements will be met by a specific material, simply because not enough is known about the effects due to surface adsorption of impurities (including adsorption of excess of constituent elements). There are, however, some useful guidelines.

The flatness/perfection of a low-energy (close-packed) surface of a crystalline material depends on the energy required to form defects in it. Some insights into this can be obtained from Jackson's model[12] which demonstrates a close relationship between surface roughness during growth and entropy for transformation (i.e., volatilization in the case of vapor growth, fusion for growth from the liquid). A

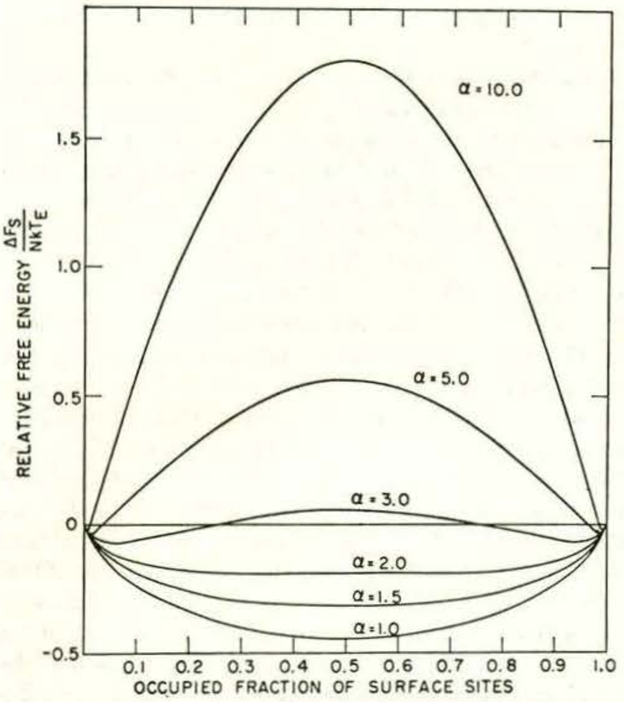

FIG. 2. Free energy of an interface vs occupied fraction of surface sites.[12]

variation of Jackson's factor α, proportional to this entropy of transformation, gives rise to marked changes in the free-energy gain or penalty that arises from surface roughness. This is shown in Fig. 2 which plots as a function of α the contribution to free energy due to surface site occupancy, that is the fraction of empty surface sites in a nearly completed layer, or of occupied sites in a layer beginning to grow (which together constitute a simple index of surface roughness). For values of α less than about 1.5 there is a minimum in this contribution at an occupancy of 0.5; in such cases the surface is always rough, giving ready nucleation and indicating that ALE would not be possible. As α increases above a value of about 2 the minimum free-energy condition rapidly moves towards a situation of extremely small occupancy or vacancy (Fig. 2). As a consequence, an increasingly smooth and perfect surface results. Since vapor–solid entropy changes are usually large this approach suggests that most vapor-grown materials should facet.

Although Jackson's model only refers to the incorporation of a single species at a growing surface, and does not appear to have been extended to more complex situations, some of its features should still be relevant. For example, the observation of marked facetting during growth is direct evidence for smooth surfaces that do not give easy nucleation; that, in turn, implies that a facetting orientation will be a requirement for the occurrence of layer-by-layer growth by ALE.

Hartmann's concept of the periodic bond chain[13] can explain many of the observed details of facetting in terms of the arrangement of chemical bonds within the material and how these intersect the surface. This idealized approach refers to a clean surface at equilibrium; the complexity of real surfaces during growth is likely to involve significant departures from that. For example, in the case of GaAs, which can give what to the eye are mirror facets on (100), Däweritz[14] has found reason for suggesting that under near-equilibrium conditions a clean but As-rich (100) surface forms minifacets bounded by a variety of planes, mainly [111]. This reduces the number of dangling bonds. It also gives a surface roughness several atomic layers in height. It is interesting to note that Theeten *et al.*[15] deduced from a simple (PBC) approach assuming atomically flat surfaces that [100] should be relatively fast growing surfaces and therefore probably nonfacetting. They also predicted that [111] surfaces of GaAs should be very slow growing, i.e., facetting, because of the difficulty of nucleation, and [110] and [113] relatively slow growing.

Experimentally the vapor growth of GaAs by the chloride technique[15] is found to be yet more complicated than would be predicted on the PBC approach modified to take into account some surface reconstruction. This is dramatically illustrated[16] in Fig. 3. Here the slowest growing orientations would be expected to be favorable for ALE. Part of the complication of this growth plot arises from the polar nature of GaAs, in which ($\bar{1}11$) and ($1\bar{1}\bar{1}$) orientations are not equivalent. In addition it has been suggested[15] that the adsorption of molecules from the gas phase (e.g., complexes containing chlorine) would be expected to modify the conclusions of a straightforward PBC approach. Such an argument, while relevant to ALE variant (ii), might not be expected to hold for variant (i). However, even with variant (i) excess of a constituent can be adsorbed on the growing surface, and so modify behavior, and, via the minifacetting mentioned previously, affect surface coverage and surface roughness. The occurrence of some kind of minifacetting may explain the abnormally small thickness increment per cycle found earlier under certain ALE growth conditions. Whether or not one can suitably modify the PBC approach into an accurate predictive tool, there is strong evidence that the kind of orientation dependent growth rate curve of Fig. 3

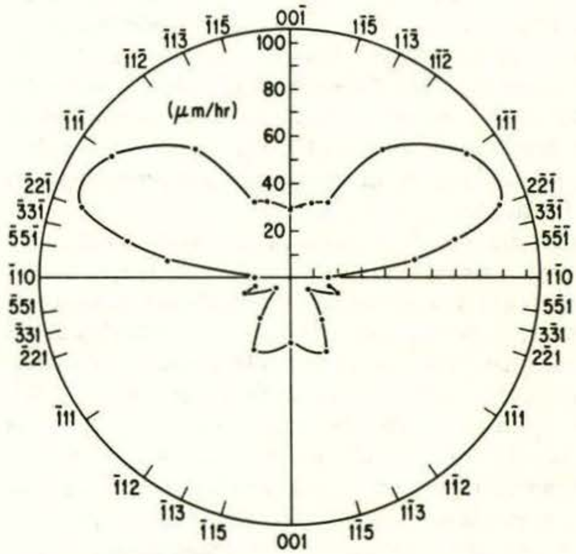

FIG. 3. Polar diagram of GaAs deposition rate vs crystallographic orientation.[16]

directly reflects the surface kinetics that govern the adsorption and incorporation of Ga and As into the growing crystal.

Considerable effort has been expended in trying to understand the detailed adsorption kinetics for GaAs surfaces, see, e.g., Refs. 16–19. However, although qualitative agreement with experiment has been obtained, as for example in Ref. 18, which deals with the effects of adsorption on the vapor growth of GaAs, it should be noted that even for such a well-characterized material as GaAs various assumptions had to be made, while some of the relevant parameters had to be plausibly estimated. It thus seems unlikely that it will be possible in the near future to predict the orientation-dependent behavior of the vapor growth of any less well-understood material. At least for the present time, therefore, whether or not a particular material might be grown by ALE must be judged semiempirically.

IV. GROWTH BY ATOMIC LAYER EPITAXY—EXPERIMENT

The cycle of alternate pulses in ALE may be repeated every 1–3 s, which yields a net growth rate of about 0.3–0.6 μm/h. Considerably longer cycle times, and hence slower growth rate, can also be used, but any significant reduction in cycle time below 1 s is unlikely, due to limited pump capacity. As already mentioned in Sec. III, the small net deposition rate may be compensated by simultaneously growing many films. An ALE reactor capable of handling a batch of substrates is illustrated in Fig. 4. Here the separation of reaction steps is accomplished by a gas flow over immobile substrates. The reactants are alternately injected into the growth chamber, and, following each reaction, are purged away by a carrier gas flow.

A. Monocrystalline deposits

The first detailed investigation of atomic layer epitaxy on single-crystal substrates was carried out at the Tampere University of Technology.[20] This employed an ultrahigh vacuum apparatus of the kind used for MBE. In order to maintain the vacuum of 10^{-7} Pa during growth limited pump capacity made it necessary to use a relatively long cycle time. The final result was a net growth rate of 0.1–0.3 μm/h. Later work[6,7,21,22] employed a new and improved MBE/ALE system, illustrated schematically in Fig. 5, and enabled faster growth to be achieved. The growth chamber incorporates three Knudsen-type effusion furnaces manufactured by Kryovak Ltd. for operation in the ALE mode (i) (and in the usual MBE mode) and two gas inlets for applying ALE variant (ii). This is built onto a VG ADES-400 electron spectrometer capable of x-ray photoelectron

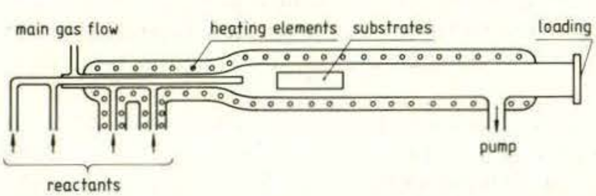

FIG. 4. Schematic diagram of a gas-flow-type ALE reactor.

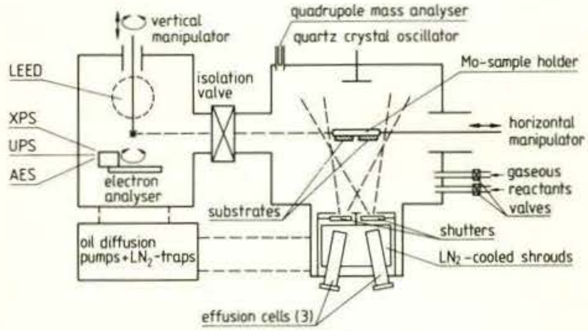

FIG. 5. Layout of an ultrahigh vacuum reactor chamber capable of ALE and MBE growth by evaporation from Knudsen-type effusion cells or by surface exchange reactions of gases from vapor sources, built on a multitechnique electron spectrometer for *in situ* characterization of films.

(XPS), Auger electron (AES), angle-resolved UV photoemission (UPS), and low-energy electron diffraction (LEED) measurements.

1. Cadmium telluride

The first material to be investigated was CdTe.[20] ALE variant (i) was used because of the rather high vapor pressures of elemental Cd and Te at elevated temperatures where the dissociative evaporation of CdTe itself would be negligibly small.[23] We note parenthetically that it might also prove possible to use ALE variant (ii), for example, with dimethyl cadmium and diethyl telluride as reactants, because these compounds have been used to grow CdTe epilayers by metal organic CVD.[24] CdTe was also chosen for investigation because of its potential importance in the areas of optoelectronics, integrated optics, and solar energy conversion. It is already used as a substrate material for $Cd_{1-x}Hg_xTe$ solid solutions and as a constituent of CdTe-HgTe superlattices, which make excellent infrared detectors for the 8–14 μm atmospheric window.[25,26]

It should be noted in passing that CdTe single-crystal substrates of high structural perfection are difficult to obtain. Other substrates, such as GaAs (100), lattice-matching InSb (100),[27,28] and (111),[27] sapphire (0001),[29] and Si (111),[30] all of which have been employed in the MBE growth of CdTe, offer viable alternatives to CdTe substrates for growth of CdTe epilayers.

ALE experiments with nonpolar (110) CdTe substrates,[20] polar (111) A and (111)B substrates,[7,21,22] as well as GaAs (100)[31] have been carried out. In order to determine an appropriate growth temperature, an amorphous Te overlayer about 1 nm thick was deposited onto the substrate at room temperature.[20] The substrate was then gradually heated to 800 K while observing the Te $M_{4,5}N_{4,5}N_{4,5}$ Auger signal at 485 eV. The intensity of this signal decreased with increasing temperature up to 540 K (see Fig. 6), above which it leveled off. This change was due to the desorption of loosely bound Te atoms in the deposit, and the constant signal in the range 550–750 K corresponded to the stable surface. Similar results were obtained for Cd. These and other similar experiments indicated that at 540 K thick amorphous deposits reevaporated at the rate of roughly 300 nm/s

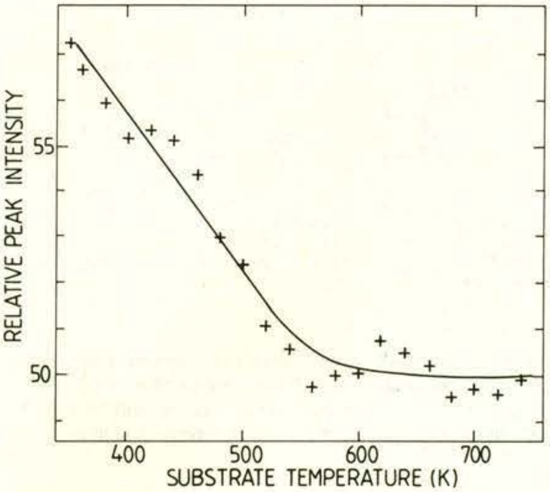

FIG. 6. Peak-to-peak height of the 485-eV Auger signal of Te for a Te deposit on a CdTe (110) substrate as a function of substrate temperature. Loosely bound Te atoms desorb at high temperature. Fluctuations in the AES peak intensities are mainly due to quick recording of the signals at short intervals while heating the sample.

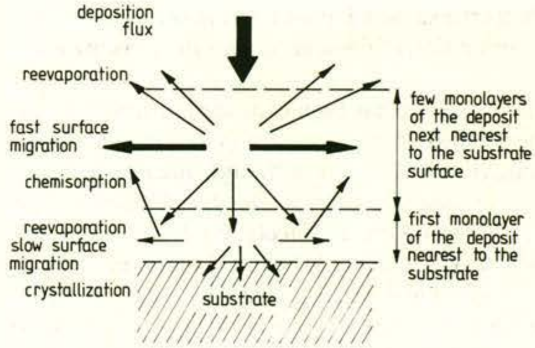

FIG. 7. Schematic illustration of the key conceptual steps associated with growth of CdTe overlayers.

for Te and 27 μm/s for Cd, confirming that ALE variant (i) was indeed operative.

With the substrate at 540 K, Cd and Te were alternately deposited as molecular beam pulses of Cd and Te_2. The deposition rate was varied from 0.01 to 0.08 nm/s, as monitored by a quartz crystal oscillator. In order to obtain a rough estimate of actual growth per cycle, films were deposited onto small pieces of molybdenum at 540 K. The Auger signals from Cd, Te, and Mo were recorded as a function of the number of ALE cycles. After 10 cycles it was found that the Mo *MNN* Auger line could no longer be detected. From this it was deduced that a film of thickness between 2 and 2.5 nm must have grown, in good agreement with the expected growth per cycle of 0.229 nm, the (110) interplanar spacing.

LEED patterns of the (110) face of the grown films showed a simple (1×1) surface unit cell. (This does not preclude reconstruction; see Ref. 32). From LEED patterns and AES and XPS spectra clean and stoichiometric single-crystal films could be obtained for T_{gr} of 480 K and above. At lower temperatures, e.g., 390 K, diffuse LEED spots suggested poor crystal structure and, usually, deviations from stoichiometry. This result was expected because the vapor pressures of elemental Cd and Te are about 10^{-4} and 10^{-8} Pa, respectively, so that some trapping of excess Te may have occurred.

It is thought that the ideal ALE model cannot fully account for LEED observations which indicate that a growing film may possess better crystal structure than the CdTe substrate.[6,21] It was partly as a consequence of these findings that an intermediate surface adsorbed layer was suggested to be present during deposition. Based on experimental studies[7] of isothermal reevaporation rates of elemental Cd and Te deposits, it was estimated that reevaporation rates of Cd and Te of this near-interface region were less than one tenth those for thick amorphous deposits of these elements. This conclusion led to a revised schematic model for the ALE process, sketched in Fig. 7. Here, the weakly bound layers just above the substrate would allow ready migration and mixing of atoms and molecules. The activation energies for reevaporation of this near-interface region were measured to be 1.5 eV for Te on CdTe (111)A and 0.5 eV for Cd on CdTe (111)B. Because the activation energies for surface diffusion are only about one-third of the bond energies,[33] i.e., 0.5 and 0.17 eV for Te and Cd, respectively, migration of the adsorbed atoms and molecules should, indeed, take place effectively in the near-interface region.

In order to study the interrelation of timing and dose of the pulses, growth experiments on CdTe were performed by varying the beam fluxes, lengths of duration of the pulses and time windows while maintaining $T_{gr} = 553$ K constant.[7] After each growth, the surface morphology was studied by a scanning electron microscope. The smoothest surface was obtained when the growth parameters were "optimized." As an example of this optimization at a relatively low net growth rate the following set of parameters may be chosen:

(a) growth rate of 0.12 nm/s of the Cd and Te deposits;
(b) length of duration of pulses from 2.5 to 2.8 s;
(c) delay times (windows) 0.5 s for the Te_2 pulse incident on CdTe (111)A and 1.0 s for the Cd pulse incident on (111) B.

In an experiment, these parameters yielded growth of a monomolecular layer of 0.37 nm per cycle in 7 s, corresponding to a net deposition rate of 190–200 nm/h.

Angle-resolved UPS, which is very sensitive to surface crystal structure and contamination, gave further information.[20] The emission peaks were sharper and of higher intensity for ALE-grown films than for the original substrate, suggesting improved quality and, probably, a smoother surface. In addition, the films grown under optimal conditions showed features that are not observed with bulk CdTe(110) unless it is cleaved in vacuum. These features of the electronic band structure were interpreted as due to the presence of occupied surface states caused by surface reconstruction.[32] They could not be seen in films grown at temperatures giving diffuse LEED spots, nor for those exposed to air, so that they were definitely associated with a rather perfect surface.

CdTe overlayers on CdTe (111)B are often better in crystal structure than those on CdTe (111)A, or on CdTe (110), as deduced from LEED. It is also noted that the sharpness of LEED patterns improves as films grew thicker,

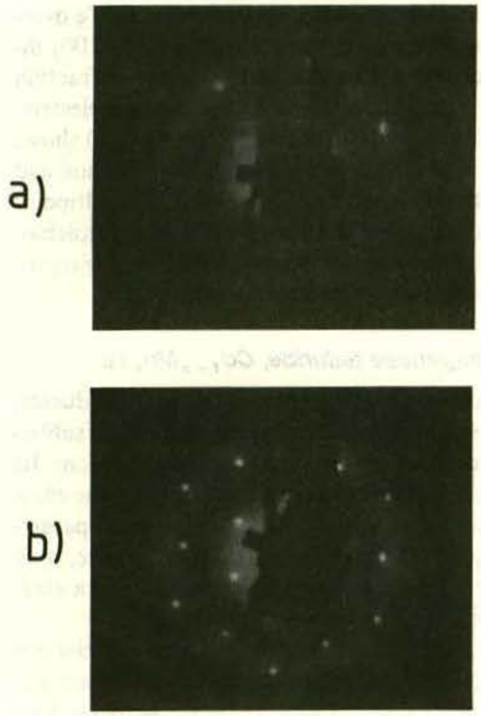

FIG. 8. LEED patterns (a) for a CdTe (111) B substrate (cleaned by Ar^+ ion sputtering then annealing at 470 K) and (b) for a 37-nm CdTe (111)A film grown on this substrate by ALE at 540 K.

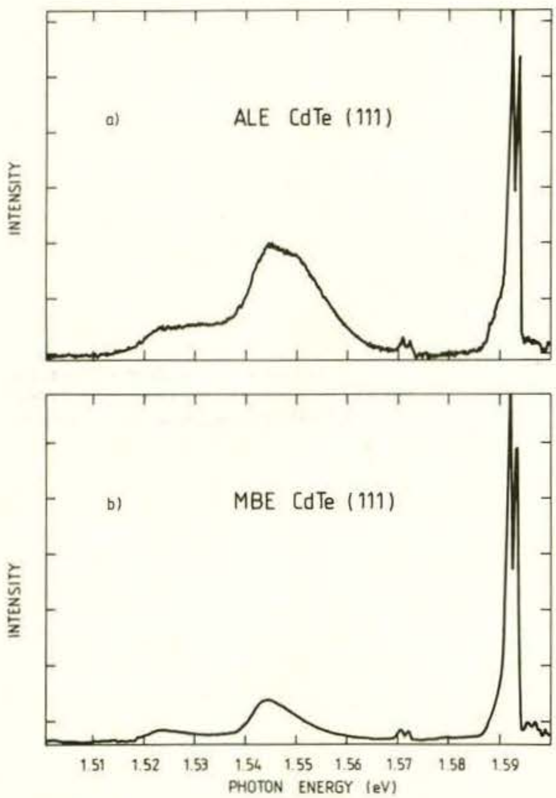

FIG. 9. Photoluminescence spectra taken at 2 K from (a) an ALE-grown CdTe/CdTe (111) sample and (b) an MBE-grown CdTe/CdTe (111) sample. These films were prepared under closely similar conditions in a CdHgTe MBE reactor at Tampere University of Technology.

at least up to 50 nm. An example of this behavior is given in Fig. 8 for growth on (111)B. However, LEED only samples local order and, therefore, small coherent areas 20–30 nm across may produce reasonably good LEED patterns. LEED is also rather insensitive to nonperiodic surface defects and dislocations. Unfortunately, high-energy electron diffraction measurements (RHEED), capable of probing large areas, have not yet been reported in the literature for ALE-grown films.

Low-temperature photoluminescence (PL) from a few ALE-grown CdTe (111)B overlayers has been measured.[34] Figure 9 shows a 2 K PL spectrum from a 1-μm CdTe film grown at $T_{gr} = 550$ K in a CdHgTe MBE reactor (at Tampere University of Technology, the reactor is not described here). There are two narrow lines just above 1.59 eV, which dominate this spectrum. They are most likely associated with radiative recombination of excitons bound to shallow acceptors (p type).[34] Their strength and sharpness provide evidence that the film is of high electrical quality. We are not able to make a definitive assignment to the broad feature ranging from 1.54 to 1.56 eV, nor to the weak doublet centered at 1.57 eV. However, a possibility arises that the broad feature is due to band-edge emission.[34] For comparison, a PL spectrum from MBE-grown CdTe prepared under closely similar conditions is also shown in Fig. 9. The two spectra are very similar. Perhaps the only difference observed is the intensity of the broad feature which is about three times greater for the ALE-grown film.

In the recent literature much attention has been paid to growth of CdTe on foreign substrates. The major limitations of employing CdTe crystals are due to the high costs and unsatisfactory grain-boundary structures. GaAs is an attractive alternative because large-area wafers of high structural perfection [dislocation densities $\approx (1\text{–}5) \times 10^4$ cm^{-2}] are readily available at a modest cost. Despite the fact that CdTe has a large lattice mismatch of 14.6% with GaAs it grows perfectly epitaxially in the (100) (Refs. 35–38) and (111) (Refs. 37, 39–41) directions on GaAs (100). The growth mechanism of CdTe on this substrate has been studied in detail by Otsuka *et al.*[37] and Datta *et al.*[42] When CdTe (100) is on GaAs (100), the (7×7) CdTe superlattice cell is almost exactly commensurate with the (8×8) GaAs cell with the two crystals being separated by a thin interfacial oxide layer. If no such oxide layer exists the growth is likely to occur in the (111) direction.[37] Massive dislocations of complex line nesting structure with line densities of 10^{11} cm^{-2} are formed in the CdTe/GaAs interface,[36] due to the lattice mismatch. However, the dislocation line density reduces gradually as the film grows thicker. In the near-surface region (≈ 100 nm) of the overlayer of thickness of a few micrometers the dislocation line density is of the same order of magnitude as in GaAs wafers.

We have grown CdTe overlayers[31] of thicknesses from 2 to 4 μm on n-type GaAs (100) substrates [oriented 2° towards (110)]. Since the growth time required for these films would have been discouragingly long by ALE alone a layer of 1–3 μm was first deposited by MBE at the rate of 0.5–1 μm/h, after which the growth was continued by ALE at a net rate of 0.2 μm/h. Figure 10 compares LEED pata)

b)

FIG. 10. LEED patterns (a) for a GaAs (100) substrate after heating at 850 K (no Ar^+ ion bombardment) and (b) for a 3.3-μm CdTe (100) film grown on this substrate at $T_{gr} = 570$ K. Primary beam energy = 45 eV.

terns for a GaAs (100) substrate and a 3.3-μm CdTe overlayer. In this example growth has occurred in the (100) direction, as indicated by LEED and by a x-ray diffraction curve shown in Fig. 11. Furthermore, a scanning electron micrograph (SEM) of the film of Fig. 10 (see Fig. 11) shows that the surface is smooth under medium magnification and comparable to that obtained usually by MBE. A multipoint AES analysis indicates that the film is uniform and stoichiometric all over the film area (of about 0.5 cm^2), being reproducible to within a few parts per thousand.

2. Cadmium manganese telluride, $Cd_{1-x}Mn_xTe$

This solid solution is a diluted magnetic semiconductor, also known as a semimagnetic semiconductor, whose sublattice is partly made up of the substitutional magnetic ions. Its ternary nature permits one to vary the energy gap, the effective mass, the lattice constant, and other physical parameters by alloying Mn.[43–45] It has interesting magnetic, optical, and magneto-optical properties,[46] for example, a giant Zeeman splitting[47] with exotic consequences.[48]

Manganese is an incongruently evaporating element having a low vapor pressure of 1.8×10^{-15} Pa, compared to 1.3 Pa for Cd and 8.3×10^{-2} Pa for Te, at $T_{gr} = 540$ K. One might therefore expect it to be impossible to make use of ALE variant (i). This problem has been circumvented by

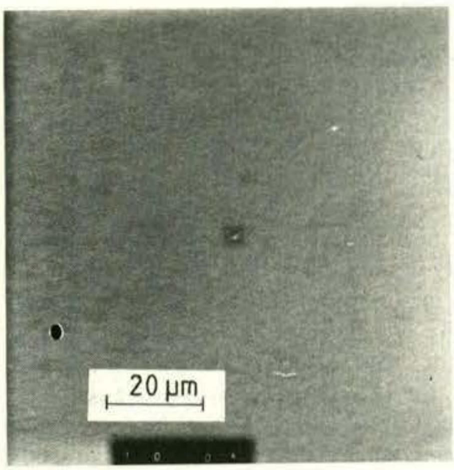

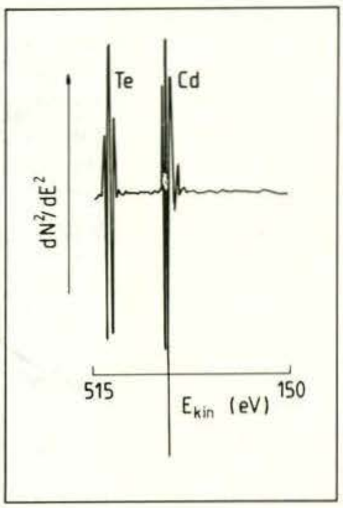

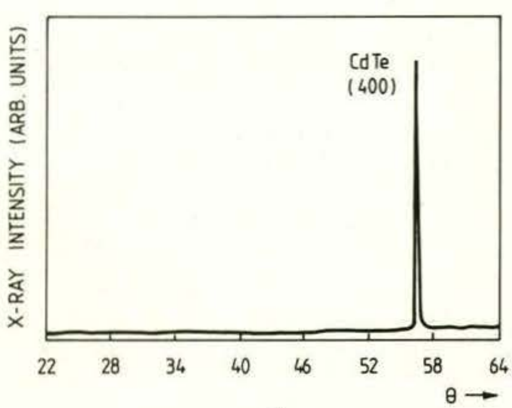

FIG. 11. (a) Scanning electron micrograph, (b) AES spectrum, and (c) x-ray diffraction for a 3.3-μm CdTe (100) overlayer on GaAs (100) of Fig. 10.

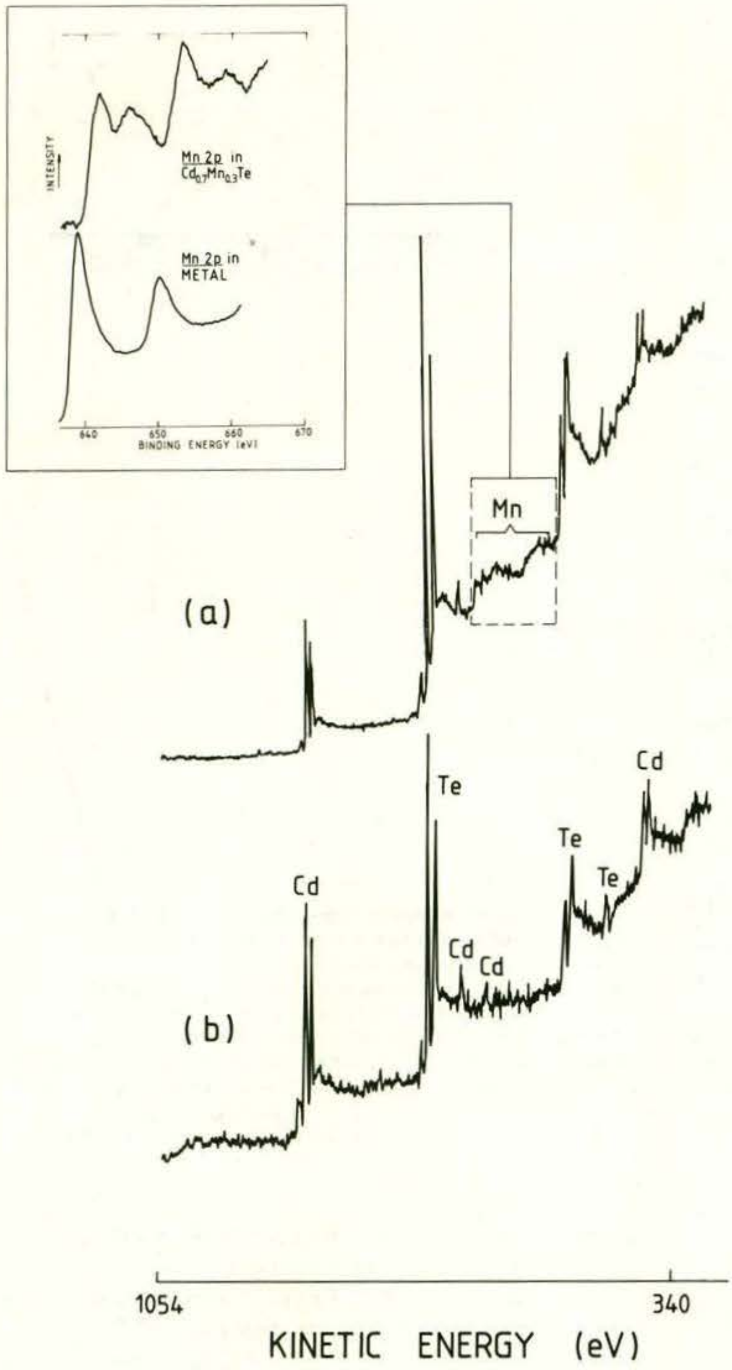

FIG. 12. X-ray photoelectron spectra (a) for a $Cd_{0.7}Mn_{0.3}Te$ (111) overlayer and (b) for a CdTe (111) overlayer. The inset shows precision measurements for the Mn $2p$ core level emission from $Cd_{0.7}Mn_{0.3}Te$ and from a metallic Mn overlayer grown on this compound.

careful control of the amount of Mn during deposition. Two different methods were used[22]:

(a) The pulsed beams of Cd and Mn were generated simultaneously by opening and closing the effusion cell shutters at the same time, with the relative Cd and Mn beam intensities set at a fixed value (e.g., 10:1);

(b) The beam intensities of Cd and Mn were equalized but the duration of the Cd pulse was made much longer than that of the Mn pulse (e.g., by a factor of 10).

It is then clear that the mole fraction x is determined by the intensity and the length of duration of the Mn pulse. An interesting feature in this stepwise growth is that when the Mn pulse is adjusted to produce a coverage less than one full atomic layer, a fixed value of $x < 1$ is always obtained per cycle; excessively arriving Cd and Te_2 or variations in these fluxes (within certain limits) do not alter x. On the contrary, MBE-type evaporation results in continuous layer growth x being determined by the *relative* concentration of Mn, Cd, and Te_2 in the vapor phase near the sample surface; any variation in the beam fluxes is reflected in x. We should note, however, that this particular ALE variant cannot be used to grow any larger film than that obtained by MBE because the opening of the cones of molecular beams is limited by geometric factors similarly to ALE and MBE.

$Cd_{1-x}Mn_xTe$ films with x ranging from 0 to 0.9 have been successfully grown by ALE on CdTe (111)B substrates at $T_{gr} = 540$ K.[22] The pulse length was varied in different experiments from 10 to 20 s for Cd and Te_2 and from 2 to 20 s for Mn. The beam intensities were chosen to correspond to the deposition rates of 0.05–0.10 nm/s for Cd and Te_2 and 0.01–0.04 nm/s for Mn. In all cases less than a monolayer of Mn was deposited in each cycle.

The $Cd_{1-x}Mn_xTe$ films were found to retain essentially their zinc-blende structure up to at least $x = 0.9$, in sharp contrast to bulklike crystals. We would like to note in this context that even pure MnTe overlayers of a zinc-blende form, when grown on appropriate substrates, are conceivable. Furdyna[49] suggested that there exist well lattice-matched substrates, such as $Cd_{0.65}Zn_{0.35}Te$ and $InSb_{0.77}P_{0.23}$ on which MnTe of the zinc-blende structure might be anchored.

Little work has been done so far on spatial distribution of magnetic ions of semimagnetic semiconductor films. One way of studying this question is to measure x-ray photoelectron spectra of the films. Figure 12 shows Mg*Kα*-XPS of pure CdTe (111) and $Cd_{0.7}Mn_{0.3}Te(111)$ grown on CdTe (111)B. It can be seen that upon alloying Mn a large reduction in relative intensity of the Cd $3e_{3/2,\ 5/2}$ doublet occurs and the Mn $2p_{1/2,\ 3/2}$ lines appear. High-precision measurements shown in the inset of Fig. 12, where XPS spectra of the $Cd_{0.7}Mn_{0.3}Te$ overlayer and a 2-nm metallic Mn overlayer deposited onto the $Cd_{0.7}Mn_{0.3}Te$ are compared with each other, provide closer insight into substitutional disorder of the sublattice. The chemical shift of 2.6 eV of the leading Mn $2p_{5/2}$ peak, the line broadening, the presence of a satellite structure, and the absence of a metallic Mn signal in the compound spectrum provide evidence that manganese is indeed a constituent of random $Cd_{0.7}Mn_{0.3}Te$ with no significant metallic clusters.

A LEED pattern for an ALE-grown $Cd_{0.82}Mn_{0.18}Te$ (111) epilayer of 30-nm thickness on CdTe (111) is shown in Fig. 13. The surface is well ordered, exhibiting sharp (1×1) LEED spots with low background intensity.

Figure 14 shows a schematic real-space energy band diagram of an ALE-grown unintentionally doped CdTe–$Cd_{0.6}Mn_{0.4}Te$ (111) multiquantum-well heterostructure. Electronic valence-band features of these two component layers were studied by measuring angle-resolved UV photoemission. Apart from differences in details of emission from the valence bands no measurable valence-band offset was observed on alloying Mn (for determining band off-sets by electron spectroscopy, see e.g., Ref. 50). Thus the difference

FIG. 13. LEED pattern of a 30-nm $Cd_{0.82}Mn_{0.18}Te$ (111) film deposited onto a 37-nm (111) buffer layer on CdTe.

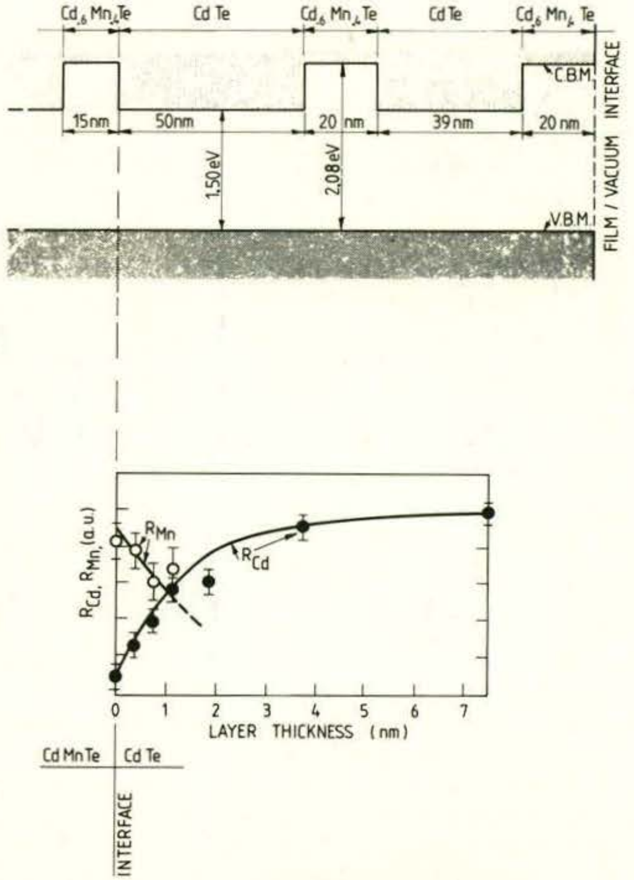

FIG. 14. Schematic real-space energy band diagram of a $Cd_{0.6}Mn_{0.4}Te$–CdTe multiquantum-well heterostructure grown by ALE (upper panel). The valence-band maximum (VBM) remains unaffected on alloying Mn to within an experimental accuracy of 50 meV investigated by angle-resolved photoemission; the difference in band gaps influences the conduction-band minimum (CBM) alone. The lower panel shows a study of the interface at the position indicated by the vertical line. This study was based on measurements of the peak-to-peak intensity ratios of Cd *MNN*, Mn *LMM*, and Te *MNN* Auger transitions; $r_{Cd} = I_{Cd}/I_{Te}$ and $R_{Mn} = I_{Mn}/I_{Te}$. The solid curves are calculated assuming that the interface is sharp and growth occurs in a layer-by-layer fashion, one molecular layer per cycle.

in the band gap E_g at the interface affects only the conduction-band minimum, as illustrated in Fig. 14.

The CdTe/$Cd_{0.6}Mn_{0.4}Te$ (111) interface was studied in a nondestructive way by combining the ALE and AES techniques. Very thin overlayers of CdTe were deposited onto $Cd_{0.6}Mn_{0.4}Te$, and Mn *LMM*, Cd MNN, and Te *MNN* AES signals were measured at room as a function of overlayer thickness. The results are shown and compared with theoretical estimates for relative signal intensities in Fig. 14. The solid curves represent the calculated behavior of Cd *MNN* and Mn *LMM* peak-to-peak intensities relative to Te *MNN* peak-to-peak intensity, $R_{Cd} = I_{Cd}/I_{Te}$ and $R_{Mn} = I_{Mn}/I_{Te}$, respectively, on the assumption that the junction is sharp. In other words, no interdiffusion of Mn or other grading effects are assumed to occur in the interface region. Furthermore, the well-known law of exponential decay of low-energy electron signals in solids was applied. The inelastic mean free paths of Cd *MNN* and Mn *LMM* electrons were taken to be 1.4 and 1.9 nm, respectively. Judging from the measured and calculated behavior of the intensity ratios one may conclude that the interface is extremely sharp, possibly of an order of atomic diameter. For comparison, by the standard AES–ion milling technique[51] the interface region of MBE-grown $CdTe/Cd_{1-x}Mn_xTe$ heterojunctions with x ranging from 0.20 to 0.53 has been found to be as large as 10 nm. Such a graded junction is an artifact which arises from an intermixing and cratering of the junction region during ion bombardment.

3. Gallium arsenide, GaAs

Nishizawa et al.[9,11] have described the growth of GaAs using ALE variant (ii). Trimethyl gallium (TMG) and AsH_3 were cycled alternately over a single-crystal substrate, using the reaction

$$Ga(CH_3)_3 + AsH_3 \rightarrow GaAs + 3CH_4.$$

The apparatus used is shown in Fig. 15. Arsine was admitted at a pressure of 10^{-4}–10^{-5} Pa for times of 2–200 s, then evacuated. A standard cycle of AsH_3 20s, evacuated for 3s, TMG 4 s, evacuated for 3 s (20, 3, 4, 3) was adopted (see Fig. 16). AsH_3 pressure was usually 7×10^{-3} Pa, TMG admittance was varied. It was found possible to obtain ALE growth at temperatures between 720 and 970 K.

The thickness of deposit grown per cycle d varied quite markedly with the amount of TMG admitted to the apparatus in each cycle. From the initial brief publication[11] d saturated at about 0.55 nm for $T_{gr} = 870$ K, as shown in Fig. 17. This corresponds to about two layers of GaAs per cycle on (100). As would be expected for the ALE mode of growth, d remained constant over large numbers of cycles, as shown in Fig. 18 which corresponds to a TMG dosage of about 10^{-2} Pa 1/s, and a d value of 0.4 nm. While the constancy appears to confirm that ALE does occur, the variation of d with the amount of TMG admitted per cycle must presumably indicate that even an incomplete coverage can lead to growth in the ALE mode, while, as already noted, sufficient TMG can allow up to two GaAs (100) layers to form per cycle even though this is not too readily explained on the simple theory presented in Sec. III. In their later work Nishizawa *et al.*[9] found much smaller d values by lowering the growth temperatures and increasing the TMG dosage. At $T_{gr} = 770$ K, d was found to saturate at a value very slightly below the 0.283-nm characteristic of a true monolayer of GaAs on (100); i.e., the simple ALE growth model was well obeyed.

One problem with the reaction between TMG and AsH_3 is that its rate falls off rapidly below 870 K apparently because of the energy required to dissociate arsine. Nishizawa[52] showed that it was possible to use UV radiation from a high-pressure Hg lamp or an excimer laser to alleviate this source of difficulty. Growth could be obtained down to temperatures as low as 560 K. This appears to be a true enhancement of reaction by the radiation, and not an effect due to heating—any temperature rise of the substrate caused by the radiation would be no more than about 1 K. It was also found that below 870 K the growth thickness per cycle decreased quite sharply for constant TMG dosage. Even at very low d values, however, a constant growth per cycle was maintained.

Some electrical results have been quoted by Nishizawa *et al.*[9] The films produced at low temperatures, ~620 K, were p type, with hole concentrations of the order of 10^{19} cm^{-3}. This high defect concentration was attributed to the incorporation of carbon. Some improvement on this was obtained by using triethyl gallium, (TEG) which still gave p-type material but with carrier concentration of the order of 10^{18} cm^{-3}. Most recently, Nishizawa[52] reported on carrier concentrations below the 10^{17} cm^{-3} level. No results have

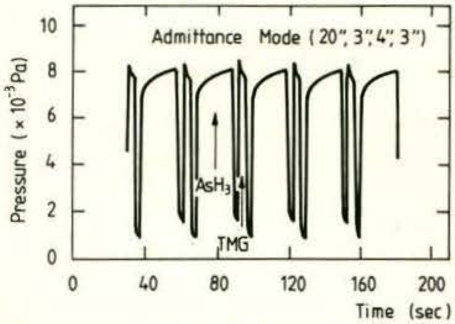

FIG. 16. Gas pressure in growth chamber of Fig. 13 during standard ALE cycles (20, 3, 4, 3 s).

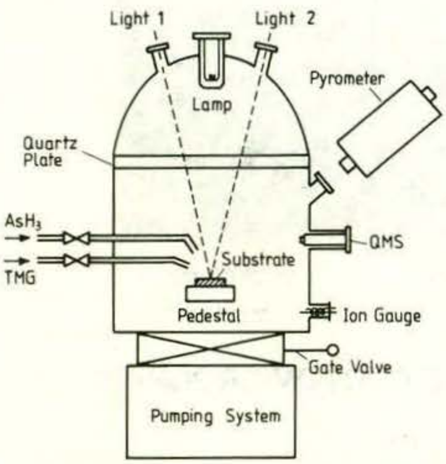

FIG. 15. Schematic drawing of equipment for atomic layer epitaxy of GaAS.[9,11] Lights 1 and 2 are for photoexcitation (see text). The lamp is for heating the substrate (QMS stands for a quadrupole mass spectrometer).

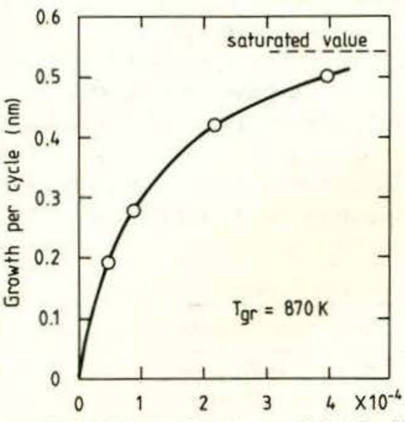

FIG. 17. Thickness per cycle of GaAs as a function of TMG admittance.

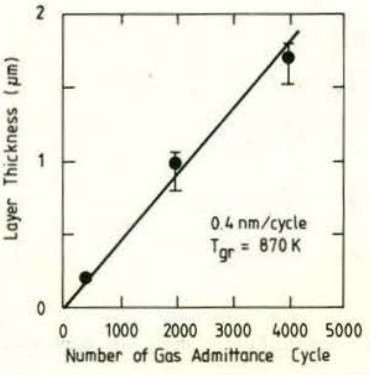

FIG. 18. Thickness of GaAs grown at 870 K vs number of ALE cycles (20, 1, 4, 1 s).

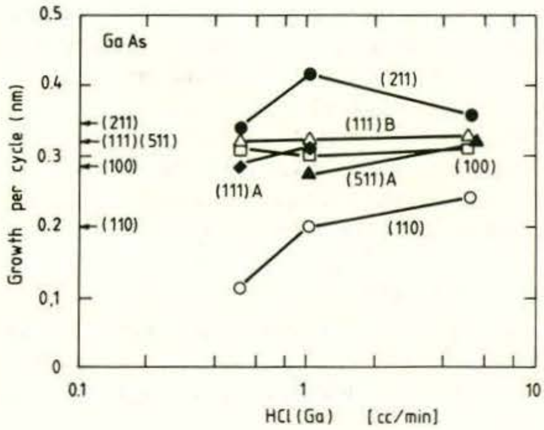

FIG. 20. Growth rate per cycle for GaAs overlayers as a function of flow rate of HCl. T_{gr} = 820 K (figure courtesy of A. Usui).

been reported for material grown at higher temperatures, or from higher alkyls e.g. tri-isobutyl gallium, either (or both) of which might lead to still lower carbon incorporation.

Usui and Sunakawa[10] at Nippon Electric Corp., Japan, have also prepared GaAs by ALE. They employed a dual growth chamber reactor in hydride vapor-phase epitaxy. The principle of his growth system is illustrated in Fig. 19. The substrate was exposed alternately to GaCl and As_4 by switching its position between the two chambers (the AsH_3 vapor stream was interrupted during the substrate transfer). The period of the cycle was 60 s but considerably shorter cycles could also be applied.

The growth thickness per cycle for several substrate surfaces was studied as a function of HCl(Ga) flow rate at T_{gr} of 820 K. The d values thus obtained remained almost constant independent of the flow rate in the range from 1 to 5 cm^3/min and closely corresponded to the thickness of a monolayer on each surface (see Fig. 20).

The films were monocrystalline, as revealed by reflection high-energy electron diffraction (RHEED) measurements, with completely mirrorlike surfaces (Fig. 21). No oval defects typical of MBE-grown GaAs were present. Furthermore, it is believed that ALE growth reduces the number of EL2 deep traps, but this has not yet been demonstrated.

Of particular importance was the observation[10] that selective growth at windows of SiO_2 masks on GaAs did not show any significant enhancement in d. This result implies that ALE might be suitable for selective epitaxy.

It is also interesting to note that preparations for growth of III-V mixed crystals by ALE are under way at NEC. Preliminary results on InGaP have already been obtained. They are found to be very encouraging.[10]

ALE growth of GaAs and AlAs from metalorganic (TMG and TMA, respectively) and hydride sources has

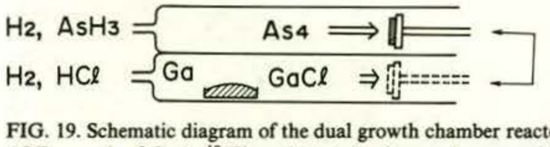

FIG. 19. Schematic diagram of the dual growth chamber reactor used for ALE growth of GaAs.[10] The substrate is alternately exposed to the two reactants (figure courtesy of A. Usui).

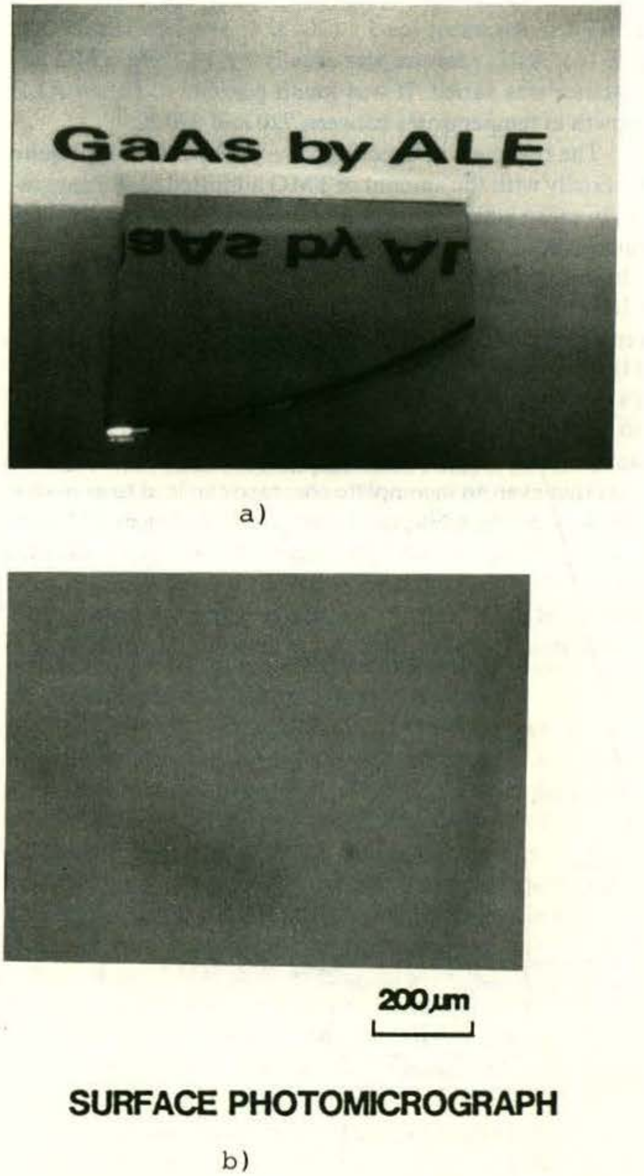

FIG. 21. (a) Photograph of a GaAs (100) film grown by ALE.[10] (b) Scanning electron micrograph of the film exhibiting no oval defects (figure courtesy of A. Usui).

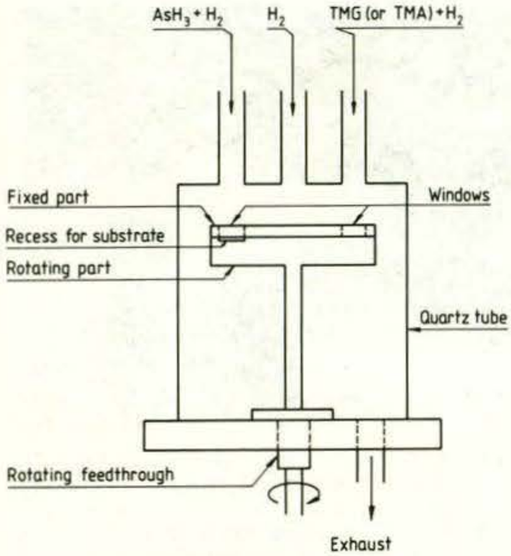

FIG. 22. Schematic diagram of the growth chamber and susceptor of ALE (Ref. 53) for preparing GaAs and AlAs. The susceptor consists of a fixed part, a rotating part, and a recess (in the rotating part) which holds the substrate. The H_2 flow in the middle tube helps prevent mixing of the reactants.

been reported by Bedair *et al.*[53] Their growth chamber (see Fig. 22) has a simple, ingeniously designed structure which may permit one to grow several samples at the same time in a cyclic fashion. The susceptor incorporates a shuttering action which allows successive exposure to streams of gases from two sources, viz., from $AsH_3 + H_2$ and TMG + H_2 for growth of GaAs, or $AsH_3 + H_2$ and TMA + H_2 for growth of AlAs. A large flow of H_2 in the middle tube is designed to prevent mixing of the reaction gases from the adjacent tubes. When the substrate is rotated away from the growth (window) position by a rotating part, most of the boundary layer will be sheared off by a fixed plate placed above the rotating part facilitating an almost immediate termination of exposure of the substrate to the input flux. In the experiments, one complete cycle was performed in about 10 s; T_{gr} for growth of GaAs and AlAs was in the range from 830 to 870 K.

The GaAs and AlAs overlayers prepared in this way on GaAs (100) substrates were single crystals, as deduced from transmission electron micrographs. Photoluminescence measured at 77 K of 100 cycles of ALE-grown GaAs sandwiched between layers of MOCVD-grown $GaAs_{0.97}P_{0.03}$ showed a full width at half-maximum of 11 meV, indicating that the sample was of a good electrical quality.

B. Polycrystalline and amorphous deposits

Most of the published papers on ALE are concerned with polycrystalline and amorphous deposits. These arise mainly from the use of amorphous substrates. In part, poor crystal structure may be due to carrying out deposition at temperatures that are only a small fraction of the absolute melting point of the material concerned, so that surface mobility of adsorbed species would be small or negligible. It is possible that many materials in this section could be grown as epitaxial layers if single-crystal substrates and higher growth temperatures were used.

The various materials grown as polycrystalline or amorphous films using ALE cycling will be listed in turn.

1. Zinc sulfide

This is the most widely studied material for ac EL thin-film displays. The growth and properties of thin films of ZnS and ZnS:Mn fabricated by ALE variant (ii) have been the subject of many investigations (see, for example, Refs. 2, 54–63. Either zinc chloride and hydrogen sulfide via the sequential exchange reaction:

$$ZnCl_2 + H_2S \rightarrow ZnS + 2HCl \, (600 < T_{gr} < 800 \text{ K}), \quad (1)$$

or anhydrous zinc acetate and hydrogen sulfide[54] via the reaction

$$Zn(CH_3COO)_2 + H_2S \rightarrow ZnS + 2CH_3COOH \, (520 < T_{gr} < 620 \text{ K}) \quad (2)$$

can be used. The occurrence of reaction (1) was demonstrated by straightforward *in situ* AES measurements[4] (see Fig. 23). The spectra shown were taken for a glass substrate which was exposed alternately to pulses of $ZnCl_2$ and H_2S under UHV conditions. The reactions were found to leave no traces of Cl or other impurities within the detection limit of AES. By contrast, ZnS grown in a gas-flow reactor of Fig. 4 from the same reactants exhibits traces of Cl and C.

Tammenmaa *et al.*[54] used reaction (2) to grow ZnS on glass. The maximum growth rate achieved was 0.26 nm per cycle, which corresponds to 6/7 of the lattice spacing of 0.312 nm in the preferential (111) growth direction. They proposed that $Zn(CH_3COO)_2$ forms multinuclear compounds in the vapor phase. Chemisorption of these species on the substrate surface leads to high coverages and, accordingly, to the relatively high growth rate observed.

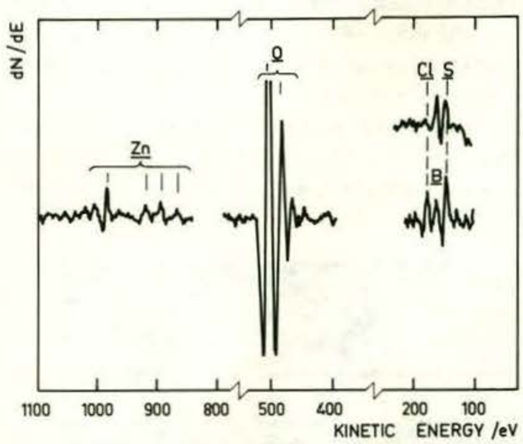

FIG. 23. Auger electron spectra showing an occurrence of stepwise growth of a ZnS film on a glass substrate via surface exchange reactions. The spectra were taken at two successive phases of a deposition cycle. The wide-range scan (100–1100 eV) in the middle was recorded after exposing the substrate to a $ZnCl_2$ pulse; Cl is chemisorbed on the surface as indicated by the appearance of the Cl AES peak. The uppermost spectrum (100–200 eV) on the right-hand side shows the absence of Cl after a pulse of H_2S which completes the cycle, yielding a growth of a ZnS molecular layer. Oxygen and boron signals originate from the glass substrate.

Tammenmaa *et al.*[54] have also carried out doping experiments in connection with growth of ZnS via reaction (2), using volatile complexes of Eu, Tb, and Tm. Photoluminescence measurements at room temperature showed that Tb^{+3} ions gave a clear PL spectrum with green emission peaking at a wavelength of 547 nm. Intensity was found to increase with Tb concentration up to 1.5 at. %. In comparison with the yellowish-orange emission (peaking at $\lambda \approx 580$ nm) from Mn^{+2}, the most common activator in ZnS, emission from Tb^{+3} was very small.

The microstructure of ALE samples from Lohja, observed by the TEM technique exhibited no fine-grained region at any thickness.[64] Fig. 24 shows a typical cross section of ZnS layers deposited onto amorphous Al_2O_3. Very pronounced columnar grain growth occurred with many grains extending from the bottom to the top of the layer. Selected area x-ray diffraction curves[56,58] showed that the films had a cubic or hexagonal polytype structure for growth in the temperature range from 300 to 570 K. The specific orientations were (111) for the cubic structure and (00.2) for the hexagonal structure which consisted predominantly of a 2H phase. The hexagonality increased remarkably in the range from 630 to 770 K. The degree of preferred orientation of microcrystallites at $T_{gr} = 770$ K was so high that one-half of the (00.2) poles were aligned within 7° of the substrate normal.

The substrate material was also found to influence the texture. The highest degree of orientation was obtained with films deposited onto a amorphous Ta_2O_5 (or Al_2O_3) buffer layer of thickness of about 50 nm grown on a glass substrate. Insertion of a microcrystalline SnO_2 layer between the glass and the Ta_2O_5 (or Al_2O_3) caused some reduction in the degree of preferred orientation.

The crystallite size varied as a function of film thickness. Typically, for films thicker than 200 nm prepared at $T_{gr} = 770$ K, the length of coherently diffracting domains in the direction normal to the surface ranged from 40 to 120 nm with a size distribution maximum at 100 nm. It is noteworthy that the mean grain diameter parallel to the film plane seen by TEM (Fig. 24) was also about 100 nm. This agreement between x-ray diffraction and TEM suggests that the columnar grains are made up of single crystals mainly of a hexagonal structure with preferential (00.2) orientation obtained at high T_{gr}.

ZnS films grown from zinc acetate at $T_{gr} = 560$–650 K exhibited the average crystallite sizes of 40–80 nm, depending on the film thickness.[63] Electroreflectance studies[65] indicated that two crystal phases, cubic and hexagonal, coexist in these films with the cubic structure predominating at the lower end of the T_{gr} range.

FIG. 25. Half-page matrix display module for personal computers. The light-emitting layer of ZnS:Mn is sandwiched between two dielectric layers of mixed Al_2O_3–TiO_2 grown by ALE. The transparent front electrode is ITO made by sputtering. The back electrode can be either ITO or aluminum. The structure is protected by a passivation layer of Al_2O_3; black printing is applied on top of the passivation layer to increase contrast.

It is thus concluded that crystal structure of ZnS films depends both on growth temperature and on source materials. The substrate has also an influence on the specific orientation of crystallites.

The dislocation density in ZnS films grown at 770 K was found[58] to be about 10^{10} cm^{-2}. This is an order of magnitude lower than the dislocation density in ZnS grown by electron beam evaporation.[60]

The ZnS:Mn films used by Lohja in their ac thin-film EL displays (see Fig. 25) exhibit a maximum luminance of 3000 cd/m² at 1 kHz. An EL external efficiency of about 2 lm/W obtained at 1 kHz has been observed.[66] At very high frequencies the external efficiency may rise up to 8 lm/W which is probably the highest efficiency attained for active layers of ZnS:Mn grown by any technique. These displays also require the introduction of dielectric layers, e.g., Al_2O_3, again grown by ALE. Uniform pinhole-free deposits of ZnS and dielectric layer materials can be obtained over very large areas—250 × 150 mm² glass substrates are routinely used at Lohja.

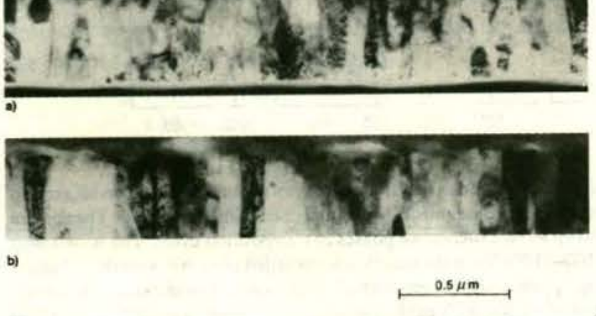

FIG. 24. Transmission electron micrographs of ZnS:Mn films grown on amorphous Al_2O_3 by ALE at Lohja Corp. (a) Corning 7059 glass substrate; (b) soda lime glass substrate.

2. Zinc telluride

ZnTe films grown from elemental Zn and Te exhibit smooth and featureless surfaces. X-ray diffraction measurements revealed that the films tended to crystallize preferentially in the (111) direction.[5] An interesting observation is that in a comparison of x-ray diffraction curves of the films grown in UHV by MBE and ALE as a function of T_{gr}, the ALE-grown films show a weaker temperature dependence of the texture than those grown by MBE. That reasonably close control of stoichiometry was maintained during ALE growth could be deduced from XPS and AES spectra.[4]

3. Oxides

Zinc acetate and water vapor have been used as reactants for growing ZnO.[54,59] The following reaction appeared to hold:

$$Zn(CH_3COO)_2 + H_2O \rightarrow ZnO + CH_3COOH \ (560 < T_{gr} < 630\ K). \quad (3)$$

The growth rate was typically 60 nm/h, and thus one-fifth of the growth rate observed in most cases for ZnS. X-ray diffraction revealed that the ZnO films were of rather poor crystallinity. Presumably this was because ZnO is a more refractory material than ZnS, so that the surface mobility of atoms at 600 K would be rather small (see comments at beginning of Sec. IV).

Growth of Ta_2O_5 by ALE variant (ii) has been realized via the reaction

$$2TaCl_5 + 5H_2O \rightarrow Ta_2O_5 + 10HCl \ (T_{gr} \approx 770\ K). \quad (4)$$

That this exchange reaction in fact occurs has been demonstrated by *in situ* AES measurements[4] of a substrate which was exposed alternately to vapor pulses of $TaCl_5$ and H_2O. Cl was seen in AES after each pulse of $TaCl_5$ but was always removed by a subsequent pulse of H_2O. Ta_2O_5 layers are amorphous (again Ta_2O_5 is a refractory material with a very high melting point). It should be noted that the extremely low vapor pressure of Ta at 770 K would prevent ALE variant (i) being employed.

Amorphous layers of Al_2O_3 are grown from anhydrous $AlCl_3$ and water vapor at $T_{gr} \approx 720$ K. They are pinhole-free and can therefore be used as an ion barrier and dielectric and passivation layers in EL devices. Although Al_2O_3 has a reasonable dielectric strength by itself, essential improvement has been achieved using a mixture of Al_2O_3 and TiO_2, prepared by ALE. SnO_2 films are grown from $SnCl_4$ and water vapor. They are noted as exhibiting some weak x-ray diffraction peaks, and so are not completely amorphous.

Work is also being done at Lohja[67] on indium tin oxide (ITO) used as a transparent conductor in displays. Resistivity of $1.6 \times 10^{-4}\ \Omega$ cm, with transmission of more than 80% has been reproducibly demonstrated over a large substrate area.

V. THE EXTENSION OF ALE TO OTHER MATERIALS

In principle it should be possible to extend ALE to a wide range of materials, even those in which one of the constituents is involatile, since there appears to be a general family of reactions that might be used for achieving ALE variant (ii). These can be summarized:

Metal halide + H_2O or oxygen→Metal oxide;
Metal halide + H_2S or sulfur vapor→Metal sulfide;
Metal halide + H_2Se or selenium vapor→Metal selenide.

One could well expect that closely related compounds to those discussed in the preceding section ($ZnCl_2$, $AlCl_3$, $SnCl_4$, and $TaCl_5$), should behave in very much the same way, for example: $CdCl_2$, $HgCl_2$, $GaCl_3$, $InCl_3$, $SiCl_4$, $GeCl_4$, $ZrCl_4$, $NbCl_5$, and also other transition metal halides, e.g., $FeCl_3$. In addition, the success of Nishizawa and Bedair *et al.* in using TMG,[9,11,53] TEG,[9,11] and TMA (Ref. 53) in the preparation of GaAs and AlAs (Ref. 53) suggests that metalorganics generally might be utilized as metal sources. Some caution may be needed here, however, not so much on account of the toxicity and pyrophoric nature of metalorganics, but with regard to their thermal stability. That must be sufficient to withstand an encounter with the hot substrate without decomposition in order that desorption of physisorbed material would occur.

It is also important to consider the second reaction component. On general thermodynamic grounds oxygen or sulfur will not react with a chemisorbed halide layer at so low a temperature as water vapor or H_2S, since such reaction would require greater free energy for the halogen to be given off as an elemental vapor than as a hydride. Since there is a major drive with electronic materials towards the use of the lowest possible temperature for material preparation, this could favor the use of the hydrides rather than the pure elements. A further important point is that H_2O, H_2S, etc. greatly resemble H_3N, H_3P, H_3As, and, as Nishizawa's work with GaAs has shown, it should be possible for such molecules to react with chemisorbed metal compounds to facilitate ALE growth of nitrides, phosphides, arsenides, etc. The first successful growth of phosphides (InGaP) has already been carried out.[10]

It should also be possible to prepare more complex materials than the relatively simple compounds discussed so far. Ferrites would serve as an example to illustrate the point. Nickel zinc ferrite could in principle be prepared from $NiCl_2$, $ZnCl_2$, and $FeCl_3$ or manganese ferrite from $MnCl_2$ and $FeCl_2$. The magnetic properties of ultrathin films of such materials remain essentially unknown and would warrant attention. It could, for example, be interesting to prepare multilayer structures of ferrites combined with nonmagnetic analogues in order to obtain direct access to effects of strain and "two-dimensionality" on magnetic properties. For development of magnetic properties, layers of good crystal perfection would be required. In order to obtain them ALE would need to be carried out on a substrate held at high temperatures, say, 0.5 of the melting point. In the case of most ferrites this might be 1000 K or more. No experiments on the ALE growth of oxides at such high temperatures has yet been attempted.

Finally the ALE approach has so far been restricted to compounds. It is conceivable that elemental materials, e.g., silicon, could be grown via chemisorption of a monolayer of, say, a chlorosilane from a stream of argon, followed by reduction of the chlorosilane in a pulse of hydrogen.

VI. CONCLUSIONS

Crystal growth in the ALE mode, whether by physical or chemical vapor deposition, is necessarily slow because individual layers of atoms are deposited with a time of the order of one second being required for each layer. Although it seems unlikely that such times could be shortened very significantly there are advantages, e.g., the feasibility of depositing several large-area films simultaneously, which make long growth times acceptable.

Where ALE might offer particularly striking advantages is in the growth of ultrathin epilayers under precise and, almost, automatic control. The technique gives a "growth per cycle" rather than a growth rate, and does so at relatively low temperatures. It therefore should enable heterojunctions with abrupt interfaces, quantum well structures and superlattices to be grown without the need for the complex and costly control systems. Additionally, ALE may provide a vehicle for investigating fundamental aspects of compound semiconductor growth. However, it still remains to be demonstrated that the perfection of structure and control of impurities and stoichiometry required of materials for electronic devices can in fact be achieved.

With regard to polycrystalline and amorphous materials, the ac thin-film EL displays made by the Lohja group have demonstrated unequivocally that ALE can be used to grow highly uniform deposits of good structural integrity both mechanically and dielectrically speaking. These qualities are of importance in many other fields, too. Application to ternary or higher compounds could also prove feasible, and low-dimensional magnetic structures might eventually be fabricated by ALE.

ACKNOWLEDGMENTS

The authors wish to thank Dr. A. Usui (NEC) and Dr. M. Tammenmaa (Helsinki University of Technology) for providing us with their results prior to publication. This work was supported in part by The Academy of Finland and The Center of Technological Development (Finland).

[1]T. Suntola and J. Antson, Finnish Patent No. 52359 (1974) and T. Suntola and J. Antson, US Patent No. 4058430 (1977); T. Suntola, A. Pakkala, and S. Lindfors, US Patent No. 4389973 (1983).

[2]T. Suntola, J. Antson, A. Pakkala, and S. Lindfors, Soc. Information Display (SID'80) Dig., 109 (1980).

[3]M. Pessa, in *Optoelectronic Materials and Devices*, edited by M. A. Herman (PWN—Polish Science Publishing, Warsaw, 1983), p. 217 and in Extended Abstracts of the First Symposium on Atomic Layer Epitaxy, Espoo, Finland, Dec. 13–14, 1984 (unpublished).

[4]M. Pessa, R. Mäkelä, and T. Suntola, Appl. Phys. Lett. **38**, 131 (1981).

[5]M. Ahonen, M. Pessa, and T. Suntola, Thin Solid Films **65**, 301 (1980).

[6]M. Pessa, O. Jylhä, and M. A. Herman, J. Cryst. Growth **67**, 255 (1984).

[7]M. A. Herman, O. Jylhä, and M. Pessa, to be published in Crystal Research and Technology (1986); for application of the generalized model of ALE variant (i) to growth of CdTe, see M. A. Herman, M. Vulli, and M. Pessa, J. Cryst. Growth **73**, 403 (1985).

[8]T. Pakkanen, M. Lindblad, and V. Nevalainen, in Extended Abstracts of The First Symposium on Atomic Layer Epitaxy, Espoo, Finland, Dec. 13–14, 1984 (unpublished).

[9]J. I. Nishizawa, H. Abe, and T. Kurabayashi, J. Electrochem. Soc. **132**, 1197 (1985).

[10]A. Usui and H. Sunakawa, The 12th International Symposium on Gallium Arsenide and Related Compound, Karuizawa, Japan, Sept. 23–27, 1985 (unpublished); A. Usui (private communication).

[11]J. I. Nishizawa, *International Conference on Solid State Devices and Materials, Kobe, Extended Abstracts* (Japan Society of Applied Physics, Tokyo, 1984), p. 1.

[12]K. A. Jackson, in *Progress in Solid State Chemistry*, edited by H. Reiss (Pergamon, Oxford, 1967), Vol. 4, Chap. 2, pp. 53–80.

[13]P. Hartman, in *Crystal Growth: An Introduction*, edited by P. Hartman (North-Holland/American Elsevier, Amsterdam/New York, 1973), Chap. 14, pp. 366–402.

[14]L. Däweritz, Surf. Sci. **160**, 171 (1985).

[15]L. B. Theeten, L. Hollan, and R. Cadoret, in *Crystal Growth and Materials*, edited by E. Kaldis and H. Scheel (North-Holland, Amsterdam, 1977), Chap. 16, pp. 196–235.

[16]D. W. Shaw, *Crystal Growth, Theory and Techniques*, edited by C. H. L. Goodman (Plenum, New York, 1974), Vol. 1, Chap. I, pp. 1–48.

[17]C. Engler and W. Lorenz, Surf. Sci. **104**, 549 (1981).

[18]J. Korec and M. Heyen, J. Cryst. Growth **60**, 297 (1982).

[19]W. Lorenz and C. Engler, Surf. Sci. **114**, 607 (1982).

[20]M. Pessa, P. Huttunen, and M. A. Herman, J. Appl. Phys. **54**, 6047 (1983).

[21]M. Pessa, O. Jylhä, P. Huttunen, and M. A. Herman, J. Vac. Sci. Technol. A **2**, 418 (1984).

[22]M. A. Herman, O. Jylhä, and M. Pessa, J. Cryst. Growth **66**, 480 (1984); M. Pessa and O. Jylhä, Appl. Phys. Lett. **45**, 646 (1984).

[23]D. L. Smith and V. Y. Pickhardt, J. Appl. Phys. **46**, 2367 (1975).

[24]I. Bhat, L.M.G. Sundaram, J. M. Borrego, and S. K. Ghandhi, in Abstracts of 1984 Fall Meeting of Materials Research Society, Boston, Mass. Nov. 26–30, 1984 (unpublished).

[25]M. A. Herman and M. Pessa, J. Appl. Phys. **57**, 2671 (1985) and references therein.

[26]J. P. Faurie, A. Million, and J. Piquet, Appl. Phys. Lett. **41**, 713 (1982); J. P. Faurier, in Extended Abstracts of The 1984 US Workshop on The Physics and Chemistry of Mercury Cadmium Telluride, San Diego, Ca, May 15–17, 1984 (unpublished).

[27]R. F. C. Farrow, G. R. Jones, G. M. Williams, and I. M. Yong, Appl. Phys. Lett. **39**, 954 (1981).

[28]R. F. C. Farrow, A. J. Noreika, F. A. Shirland, W. J. Takei, S. Wood, J. Greggi, and M. H. Francombe, J. Vac. Sci. Technol. A **2**, 527 (1984).

[29]T. H. Myers, Y. Lo, R. N. Bicknell, and J. F. Schetzina, Appl. Phys. Lett. **42**, 247 (1983).

[30]Y. Lo, R. N. Bicknell, T. H. Myers, and J. F. Schetzina, J. Appl. Phys. **54**, 4238 (1983).

[31]M. Pessa and O. Jylhä (unpublished work).

[32]C. B. Duke, A. Paton, and W. K. Ford, Phys. Rev. B **24**, 3310 (1981); J. Vac. Sci. Technol. **20**, 778 (1982).

[33]J. A. Venables, Vacuum **33**, 701 (1983); J. A. Venables, G. D. T. Spiller, and M. Hanbucken, Rep. Prog. Phys. **47**, 399 (1984).

[34]The PL spectra were measured and partly interpreted by B. Monemar at The University of Linköping, Sweden.

[35]K. Nishitani, R. Okhata, and T. Murotani, J. Electron. Mater. **12**, 619 (1983).

[36]R. N. Bicknell, R. W. Yanka, N. C. Giles, J. F. Schetzina, T. J. Magee, C. Leung, and K. Kawayoshi, Appl. Phys. Lett. **44**, 313 (1984).

[37]N. Otsuka, L. A. Kolodziejski, R. L. Gunshor, S. Datta, R. N. Bicknell, and J. F. Schetzina, Appl. Phys. Lett. **46**, 860 (1985).

[38]J. J. Dubowski, D. F. Williams, P. B. Sewell, and P. Norman, Appl. Phys. Lett. **46**, 1081 (1985).

[39]J. T. Cheung, M. Khoshenevisan, and T. J. Magee, Appl. Phys. Lett. **43**, **462** (1983).

[40]P. P. Chow, D. K. Greenlaw, and D. Johnson, J. Vac. Sci. Technol. A **1**, 562 (1983).

[41]H. A. Mar, K. T. Chee, and N. Salansky, Appl. Phys. Lett. **44**, 898 (1984).

[42]S. Datta, J. K. Furdyna, and R. L. Gunshor, Superlattices and Microstructures **1**, 327 (1985).

[43]R. R. Galazka, in *Physics of Semiconductors 1978*, edited by B. L. H. Wilson (Institute of Physics Conf. Ser. No. 43, London, 1979), p. 133.

[44]J. K. Furdyna, J. Appl. Phys. **53**, 7637 (1982).

[45]N. B. Brandt and V. V. Moshchalkov, Adv. Phys. **33**, 193 (1984).

[46]A. V. Nurmikko, R. L. Gundshor, and L. A. Kolodziejski, J. Quantum Electron (to be published).

[47]M. Dobrowolska, A. M. Witowski, J. K. Furdyna, T. Ichiguchi, H. D. Drew, and P. A. Wolff, Phys. Rev. B **29**, 6652 (1984).

[48]J. A. Gaj, R. R. Galazka, and M. Nawrochi, Solid State Commun. **25**, 193 (1978).

[49]J. K. Furdyna and J. Kossut, Superlattices and Microstructures (to be published).

[50]S. P. Kowalczyk, J. T. Cheung, E. A. Kraut, and R. W. Grant, in Proceedings of The 1985 US Workshop on Physics and Chemistry of CdHgTe, San Diego, Oct. 7–10, 1985, p. 143 (unpublished).

[51]L. A. Kolodziejski, T. Sakamoto, R. L. Gunshor, and S. Datta, Appl. Phys. Lett. **44**, 799 (1984).

[52]J. I. Nishizawa, private communication and a lecture in The 32nd National Symposium of American Vacuum Society, Houston, TX, Nov. 19–22, 1985 (unpublished).

[53]S. M. Bedair, M. A. Tischler, T. Katsuyama, and N. A. El-Masry, Appl. Phys. Lett. **47**, 51 (1985).

[54]M. Tammenmaa, T. Koskinen, L. Hiltunen, M. Leskelä, and L. Niinistö,

in Extended Abstracts of The First Symposium on Atomic Layer Epitaxy, Espoo, Finland, Dec. 13–14, 1984 (unpublished).
[55]V. P. Tanninen, M. Oikkonen, and T. Tuomi, Phys. Status Solidi A **67**, 573 (1981).
[56]V. P. Tanninen and T. Tuomi, Thin Solid Films **90**, 339 (1982).
[57]R. Törnqvist, J. Appl. Phys. **54**, 4110 (1983).
[58]V. P. Tanninen, M. Oikkonen, and T. Tuomi, Thin Solid Films **109**, 283 (1983).
[59]M. Tammenmaa (private communication).
[60]D. Thesis, H. Oppolzer, G. Ebbinghaus, and S. Schild, J. Cryst. Growth **63**, 47 (1983).
[61]J. A. Lahtinen and T. Tuomi, Acta Polytech. Scand. Appl. Phys. Ser. **138**, 97 (1983).
[62]R. O. Törnqvist, J. Antson, J. Skarp, and V. P. Tanninen, IEEE Trans. Electron Devices **ED-30**, 468 (1983).
[63]M. Oikkonen, M. Blomberg, T. Tuomi, and M. Tammenmaa, Thin Solid Films **124**, 317 (1985).
[64]L. E. Tannas, Jr., Electroluminescent Displays, Report 6475 (Aerojet Electro Systems, 1983).
[65]J. A. Lahtinen, A. Lu, T. Tuomi, and M. Tammenmaa, J. Appl. Phys. **58**, 1851 (1985).
[66]T. Suntola, International Symposium Digest, Society of Information Display, New York, April 20–21, 1981 (unpublished).
[67]T. Suntola and J. Hyvärinen, Annu. Rev. Mater. Sci. **15**, 177 (1985).